

# Wireless sensor monitoring of Paddington Station Box Corner

X.M. Xu<sup>\*1</sup>, S. Nawaz<sup>2</sup>, P. Fidler<sup>1</sup>, D. Rodenas-Herraiz<sup>2</sup>, J. Yan<sup>1,3</sup> and K. Soga<sup>1</sup>

<sup>1</sup> *Department of Engineering, University of Cambridge, Cambridge, UK*

<sup>2</sup> *Computer Laboratory, University of Cambridge, Cambridge, UK*

<sup>3</sup> *School of Electronics and Computer Science, University of Southampton, Southampton, UK*

<sup>\*</sup> *xx787@cam.ac.uk*

**ABSTRACT** This paper presents the real performance of three diaphragm wall panels on the southeast corner of Paddington Station Box during excavation, monitored using a wireless sensor network. In total, 15 LPDT displacement sensors, 12 tilt sensors, 13 relay nodes and a gateway were deployed at three different stages. Each wireless sensor node is programmed with Contiki OS using the in-built IPv6-based network layer (6LoWPAN/RPL) for link-local addressing and routing, and ContikiMAC at the medium access control (MAC) layer for radio duty cycling. Extensive testing and calibration was carried out in the laboratory to ensure that the system functioned as expected. Wireless tilt and displacement sensors were installed to measure the inclination, angular distortion and relative displacement of these corner panels at three different depths. The monitoring data reveal that the corner produced a stiffening effect on the station box, which might result in a breakdown of plane strain conditions. The network performance characteristics (e.g. message reception ratio and network topology status) and challenges are also highlighted and discussed.

## 1 INTRODUCTION

Spatial corner effects in deep excavations have been observed through traditional field instrumentation programs and numerical analyses (e.g. Ou et al. 1996; Tanner Blackburn & Finno 2007; Tan et al. 2014). The minimum D-wall deflections occurring near the pit corners during excavation were attributed to the three-dimensional stiffening effects caused by the higher stiffness at the corners. This would result in a breakdown of plane strain condition, which has been commonly adopted in engineering practice.

This paper presents real-time monitoring of the movement of three diaphragm wall corner panels in a very long and narrow station box, using a wireless sensor network (WSN). The site for the WSN deployment was an excavation for a new Crossrail station at Paddington, London, which took the form of an underground box (260m long, 25m wide and 23m deep). It is anticipated that these instrumentations would quantify the spatial corner effects, and to fur-

ther improve the understanding of the performance near the corners of large deep excavations.

## 2 WIRELESS SENSING SOLUTIONS

The monitoring instrumentation installed onto the panels consists of displacement transducers and tilt sensors. The sensing information was transmitted wirelessly (via relays as required) to a gateway, which was connected to a mobile phone network. Extensive testing and calibration of the entire system were undertaken in the laboratory prior to on-site installation.

### 2.1 Wireless solutions

The tilt and displacement sensors used in the deployment were obtained from Wisen Innovation. These devices are internally based on the AVR ATmega1281 processor and the IEEE 802.15.4-compliant AT86RF231 radio. Fifteen sensors measured displacement using an LPDT while twelve

measured tilt using Murata SCA100T MEMS inclinometers. For the thirteen relay nodes, Dresden Elektronik deRFmega128 modules were used. The gateway used a Memsic Iris mote acting as the root node and border router. This was attached to a Memsic MIB520 Gateway with data transferred over a USB connection and logged using a Raspberry Pi single board computer. Internet connectivity was provided by a 3G USB modem.

The application software running on the wireless sensor devices was developed in Contiki OS (Dunkels et al. 2004). Nodes use Contiki's standards-based IPv6 stack (6LoWPAN/RPL) for link-local addressing and routing, and ContikiMAC at MAC layer for low-power operation. A more detailed description of the software can be found in Nawaz et al (2015).

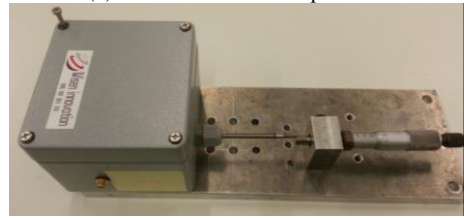
## 2.2 Wireless sensor calibration

All the wireless sensors were calibrated in the lab, using calibration platforms shown in Fig.1, a laptop and a Sky gateway mote. The tilt sensor calibration platform can achieve 1/60 degree resolution, and that of the displacement sensor calibration platform can be as much as 0.01mm. For calibration the sensors were programmed with a version of the code which used a data transmission rate of 1 second per data message. For each tilt sensor, the calibration was performed in a range of -5 degree to 5 degree for both X and Y directions, with a minimum interval of 1/60 degree. The calibration range for each displacement sensor was made from -10 mm to 10 mm, 0.01 mm minimum interval. The calibration process was repeated up to 3 times for each sensor.

Fig. 2 shows two examples of the calibration results from tilt sensor 18 and displacement sensor 04. It can be observed that the sensing data can be well characterized using the equations described in each figure. However, it was also found that there was significant discrepancy in the key characteristic parameter for each sensor. For example, the sensitivity coefficient of the displacement sensor used in this project varies from 0.03768 V/mm to 0.04256 V/mm, with a mean value of 0.0405075 V/mm. This is probably due to differences in the assembly and package of each sensor. It is therefore essential that all the sensors be individually calibrated prior to actual on-site installation.

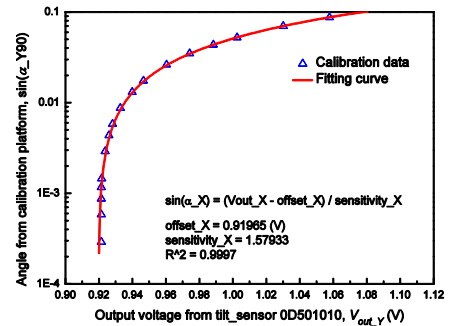


(a) Tilt sensor calibration platform

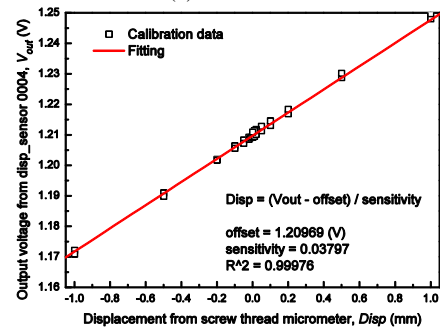


(b) Displacement sensor calibration platform

**Figure 1.** Wireless sensor calibration platforms: (a) tilt sensor; (b) displacement sensor.



(a) Tilt sensor



(b) Displacement sensor

**Figure 2.** Example results of the calibrated wireless sensors: (a) tilt sensor; (b) displacement sensor.

### 2.3 WSN Lab testing

Three lab tests in total were carried out in the laboratory to ensure that the WSN system was viable for deployment. For the first two tests, 15 wireless sensors and a gateway were tested, while for the third test 17 wireless sensors were tested. Satisfactory network performance was found for all these three tests, each lasting for around 2 weeks period.

## 3 FIELD DEPLOYMENT

A wireless sensor network was deployed in Paddington construction site in stages, including a gateway, 13 relays, 15 LPDT sensors and 12 tilt sensors.

### 3.1 Field overview

The Paddington Crossrail station is being built directly below Departures Road and Eastbourne Terrace, as marked with a red rectangle showing in Fig. 3. The construction site is bounded by Eastbourne Terrace, Bishop's Bridge Road, Departures Road/Macmillan House and Praed Street. The inset of the Fig. 3 also plots the three D-wall panels around the Southeast corner. Construction started in October 2011 and is due to be completed during 2017.

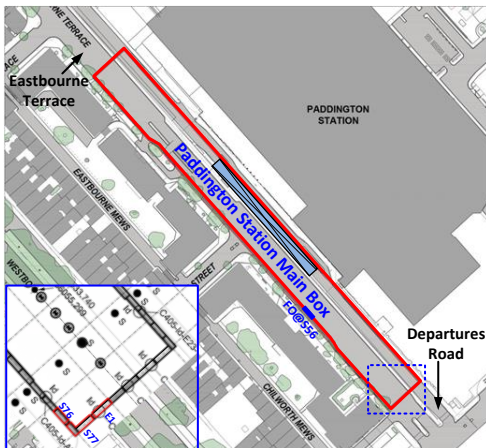


**Figure 3.** Paddington site main box site location.

The site is partially underlain by Pleistocene River Terrace Deposits (Lynch Hill Gravel), absent to the northwest of the site, over Eocene London Clay and Harwich Formation underlain by the Lambeth Group,

Thanet Sand Formation and Cretaceous Upper Chalk. Recent Langley Silt is recorded above the River Terrace Deposits to the east of Paddington Station.

### 3.2 Sensor node locations

The parameters of particular interest in this monitoring scheme are the angular distortion and inclination of L-shaped corner panel (S77), as well as the relative movement of the panels immediately adjacent to it (S76 and E1). It was intended to instrument these three panels at four different levels (namely +119.0 m, +115.5 m, +113.1 m and +107.0 m), as the excavation proceeded.

At each installation level, five LPDT sensors and four tilt sensors were to be installed, including: (1) one LPDT sensor to span diagonally across the L-shaped panel S77; (2) two LPDT sensors to span across panels S76 and S77; (3) two LPDT sensors to span across panels S77 and E1; and (4) four biaxial tilt sensors on the three panels. The detailed layout of the sensors around the corner is illustrated in Fig. 4.

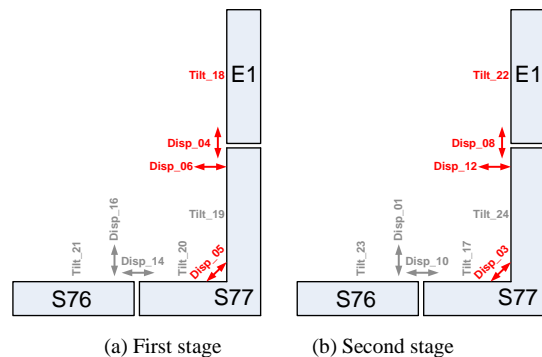


**Figure 4.** Sensor locations: (a) First stage at level +119.0m; (2) Second stage at level +115.50m.

### 3.3 Field deployment

Prior to field deployment, all the sensors were re-programmed with a deployment version of the application software, which was also tested in the lab. Each node was also suitably labelled to inform operators on site of the monitoring undertaken. To ease the installation of the LPDT sensors, a number of bespoke steel brackets were designed and manufactured at the University of Cambridge, including brackets for the diagonally mounted sensor spanning across the L-shaped panel, and others for mounting sensors

across spacing between adjacent panels. Concrete blocks were prepared in the lab to test the installation process.

A gateway and four relays were firstly deployed in Paddington construction site on 22<sup>nd</sup> January 2014. The gateway was positioned outside the station main box and adjacent to the permanent opening (see Fig. 5(a)), as it requires a power supply (110V) and good 3G signal coverage. One relay was placed on the top of panel N50 at Departures Road level, to ensure its good connectivity with both the gateway and other relays inside the main box. The other three relays were attached to panels (as indicated in Fig. 5(b)) and plunge columns at Intermediate level. As the excavation progresses and slab casts, more relays were added at Concourse level. Note that the locations for attaching relays were very limited due to specific site requirements regarding the positioning of sensing instrumentation, with the D-wall panels and plunge columns only.

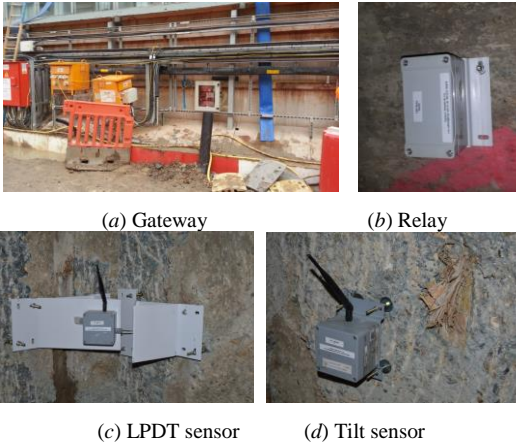


**Figure 5.** Field deployment of wireless sensor network at Paddington: (a) Gateway; (b) Relay; (c) LPDT sensor; (d) Tilt sensor.

The sensor installation at level +119.0m took place on 17<sup>th</sup> and 18<sup>th</sup> February 2014. Each sensor was attached onto a bracket using four screws, and the steel bracket was then mounted onto the D-wall using 4 concrete anchor bolts (bolt diameter 1/4 inches, minimum embedment 2 inches). The rest of sensors were installed on 14<sup>th</sup> March 2014 at level +115.5m and on 16<sup>th</sup> April 2014 at level +113.1m. Unfortunately, the installation at level +107.0m could not be realized due to the limited site access. The

layout of the entire wireless sensor network is illustrated in Fig. 6. All the sensors were removed from D-wall panels on 4<sup>th</sup> August 2014.

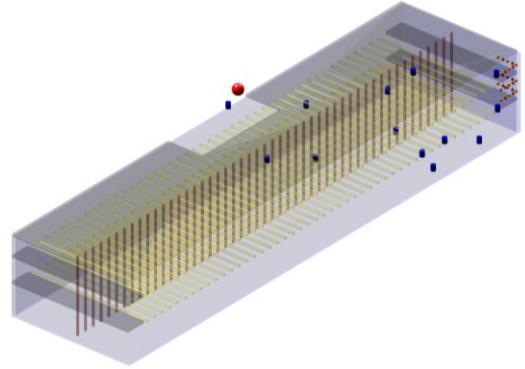


**Figure 6.** Model of Paddington station box and WSNs layout. Red sphere represents for gateway; blue cylinder for relays.

#### 4 NETWORK DYNAMICS

Fig. 7 presents the layout of the initial network topology, which is obtained from network diagnostic messages transmitted by all nodes in a periodical basis. Interestingly, it shows that sensor nodes were mainly routing messages via a far-off relay which was located on the opposite side of the station box in close proximity to the gateway.

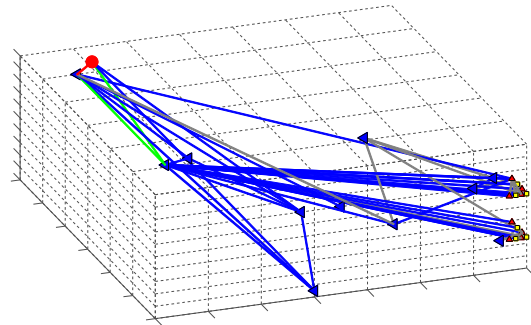


**Figure 7.** Initial network topology at Paddington (15<sup>th</sup>-19<sup>th</sup> March 2014). Link colour represents the average number of connections made to the gateway per day during the 5-day period. Grey line indicates one-two connections; blue line, between 2 and 20 connections; green line, between 20 and 200 connections; and red line, more than 200 connections.

Fig. 8 shows the message delivery ratio (MDR) for 5 individual LPDT sensors and 4 tilt sensors during the entire monitoring period. The values of MDR

for every node was obtained as the number of data messages successfully delivered to the gateway with respect to the total number of expected data transmissions. It can be observed from the figure that, the network experienced continuous connectivity problems that resulted in MDRs of below 10% in the first three months after deployment.

With the installation of two additional relays on 15<sup>th</sup> May 2014, an improvement in MDR for all sensor nodes (up to four times more) was observed (as shown in Fig. 8). Unfortunately, this improvement only lasted for around 20 days, after which the MDRs dropped again. A more detailed description and explanation of the network dynamics can be found in Nawaz et al (2015).

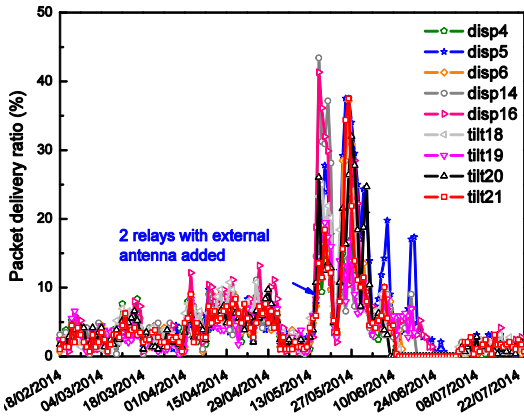
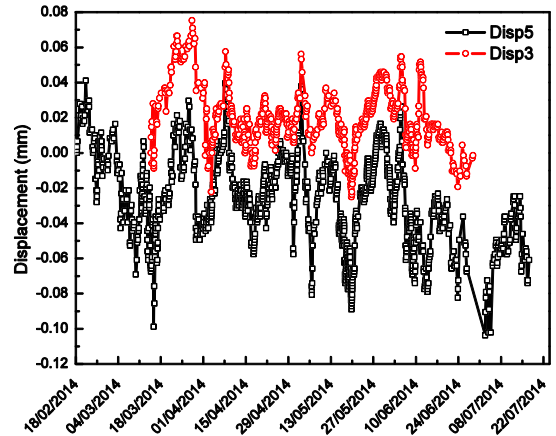


Figure 8. Packet delivery ratio at the gateway

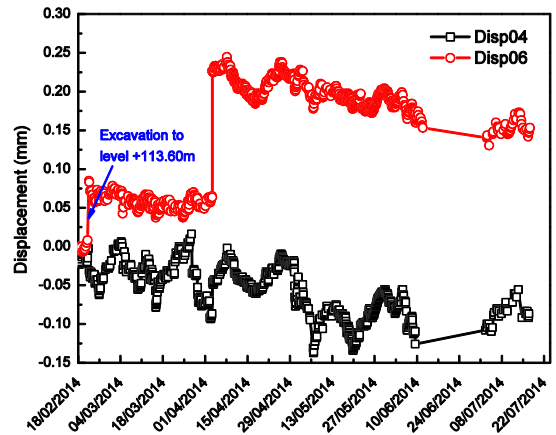
## 5 MONITORING RESULTS

Although the WSN performance was not as good as expected, the received sensing data do provide sufficient information on the movements of three instrumented D-wall panels. For example, the measured displacement and inclination from four displacement sensors and two tilt sensors (as highlighted in Fig. 5) are plotted in Fig. 9. It can be observed from the figure that: (1) the maximum displacement for the L-shaped panel S77 was around 0.10mm (as indicated in Fig. 9(a)), which corresponds to the angular distortion of about 1/2865 (0.02 degree) according to the sensor configurations. This might suggest that its extensive reinforcement may be unnecessarily, and significant cost savings may be

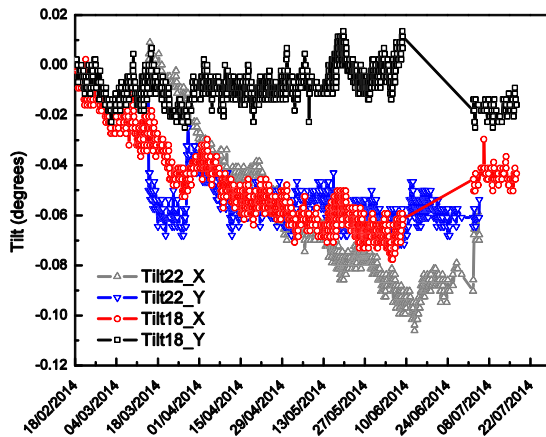
possible; (2) the construction activity induced movement between panel E1 and S77 was up to 0.233 mm, as indicated in Fig. 9(b); (3) the inclination on panel E1 was up to 0.10 degree. All the sensing data is to be further compared and analyzed with the readings from other instrumentations (e.g. FO sensing on panel S56 as highlighted in Fig. 5, inclinometers, temporary prop loads, etc.), to gain some insights into the spatial corner effects of this long and narrow pit.



(a) Displacement in panel S77 (at +119.0m & +115.5m)



(b) Displacement between panels E1 and S77 (at +119.0m)



(c) Inclination of panel E1 (at +119.0m & +115.5m)

**Figure 9.** Measured movements on instrumented D-wall panels.

## 6 CONCLUSIONS

This paper presents a performance monitoring of three D-wall panels in a long and narrow pit using wireless sensor networks. The received sensing data implies that there might be significant overestimation on the panel deformation at the corners. Further analysis is ongoing to examine their spatial corner effects. The wireless network performance in this challenging environment was not satisfactory, and there is a strong need for improvements in the robustness of wireless sensor network communication schemes for construction monitoring.

## ACKNOWLEDGEMENT

This research has been supported by Cambridge Centre for Smart Infrastructure and Construction (CSIC). We would like to thank Costain-Skanska Joint Venture (CSJV) and our industrial partner Crossrail for allowing access and instrumentation of the Paddington site. We would also like to thank Mr. Mohamad Alserdare from HS2 Ltd, Dr. Munenori Shibata from Japan Railway Technical Research Institute, Prof. Dan Zhang from Nanjing University, and Mr. Peter J Knott (CSIC) for their invaluable assistance with sensor network deployment.

## REFERENCES

- Dunkels, A., Grönvall, B. & Voigt, T., 2004. Contiki - A lightweight and flexible operating system for tiny networked sensors. *Proceedings - Conference on Local Computer Networks, LCN*, pp.455–462.
- Nawaz, S. et al., 2015. Monitoring A Large Construction Site Using Wireless Sensor Networks. *Proceedings of the 6th ACM Workshop on Real World Wireless Sensor Networks*, pp.27–30. Available at: <http://doi.acm.org/10.1145/2820990.2820997>.
- Ou, C.-Y., Chiou, D.-C. & Wu, T.-S., 1996. Three-dimensional finite element analysis of deep excavations. *Journal of Geotechnical Engineering*, 122(5), pp.337–345.
- Tan, Y. et al., 2014. Spatial corner effects of long and narrow multipropped deep excavations in shanghai soft clay. *Journal of Performance of Constructed Facilities*, 28(4). Available at: <http://www.scopus.com/inward/record.url?eid=2-s2.0-84904470556&partnerID=40&md5=47e6e5b71e5f4241e2b33720251a9f1a>.
- Tanner Blackburn, J. & Finno, R.J., 2007. Three-Dimensional Responses Observed in an Internally Braced Excavation in Soft Clay. *Journal of Geotechnical and Geoenvironmental Engineering*, 133(11), pp.1364–1373.